Seismic Behavior of Colliding Buildings, Incorporating Soil-structure Interaction and Accounting for Variability in Structural Parameters, Soil Parameters, and Seismic Action

Ikhlasse Kheira Asmouni[1*], Mohammed Mekki[1], Mohammed Bensafi[1]

[1] LM2SC Laboratory, Department of Civil Engineering, Faculty of Architecture and Civil Engineering, University of Sciences and Technology Mohamed Boudiaf, BP 1505 El Mnaouer, 31000, Oran, Algeria
[*] Corresponding author, e-mail: ikhlassekheira.asmouni@univ-usto.dz

Abstract

Pounding between buildings that are not sufficiently separated has been observed several times during earthquakes. This destructive impact may severely damage the structure and lead to its collapse. Although it is impossible to completely eliminate such losses, measures can be taken to minimize them. This article investigates the effect of the variability of structural parameters, soil parameters, and seismic action on the seismic response of two colliding buildings, taking the soil-structure interaction (SSI) into account. Two adjacent structures closely separated, modeled as inelastic lumped mass systems with different structural characteristics, were considered in this study. Both structures were modeled in the analysis using multi-degree-of-freedom (MDOF) systems, and the pounding was simulated using the modified linear viscoelastic model. The analysis was conducted in two cases: probabilistic analysis and deterministic analysis. Probability curves were established to analyze the effect of the variability of the parameters on the responses of the two colliding buildings. The comparison between the two analyses indicates that the probabilistic analysis is more precise than the deterministic analysis. It has been indicated that taking into account the variability of structural parameters, soil parameters, and seismic action is efficient in determining the realistic behavior of colliding buildings. Additionally, pounding is more critical in the case of buildings founded on very soft soil, followed by those on soft soil, then on hard soil, and finally on rocky soil.

Keywords

pounding, adjacent structures, colliding buildings, soil structure interaction, variability

1 Introduction

One of the most important natural disasters facing human society today is the earthquake disaster, which is characterized by suddenness and destructiveness. In recent years, protecting against the destructive effects of earthquakes has received more attention, particularly concerning the collisions between adjacent structures, especially during previous earthquakes such as those in San Fernando 1971 [1], Mexico City 1985 [2], Lom Prieta 1989 [3], and Bhuj 2001 [4]. Pounding was also observed in recent earthquakes, such as Christchurch (New Zealand, 2011) [5] and Gorkha (Nepal, 2015) [6]. Additionally, pounding was observed in Algeria, especially during the Boumerdes earthquake (M = 6.8) in 2003 [7]. The majority of the damages observed during these earthquakes were caused by pounding, which occurred between two adjacent structures that were located too close to each other, and the gap between them did not satisfy the minimum distance required for them to vibrate freely, see Fig. 1.

Numerous researchers have extensively investigated the phenomenon of structural pounding, considering various structural configurations and diverse ground motions. Anagnostopoulos [8] studied the pounding of buildings in series during earthquakes, where the structures were modeled as single-degree-of-freedom. The author found that the outer structures in the series responded more severely than the inner ones. Moreover, research has shown that the dynamic response of adjacent structures is significantly influenced by dynamic structural parameters such as the natural vibration period, mass, and damping. Also, a change in the structural design, the separation distance between the colliding buildings, or the ground motion excitation may lead to different results [9].

The previous investigation confirmed that the behavior of lighter and more flexible buildings is severely impacted by structural pounding during earthquakes, which can eventually lead to considerable permanent deformation
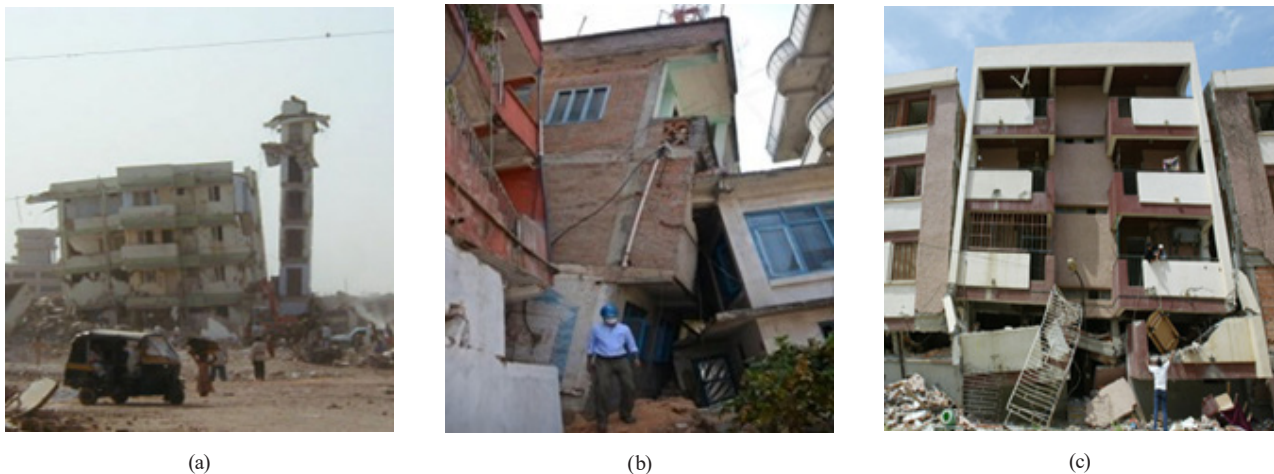
(a)   (b)   (c)

Fig. 1 Examples of buildings that were impacted by pounding in three different earthquakes: (a) Bhuj (2001), (b) Nepal (2015), and
(c) Boumerdes (Algeria, 2003)

of the structures due to elastic deformation. In contrast, heavier and stiffer buildings are nearly unaffected by collisions between structures [10, 11]. The investigations have also indicated that pounding has a negative impact on the seismic responses of closely separated buildings, and the impact increases as the separation gaps decrease.

Several mechanical devices have been used to mitigate the effects of vibrations in structures. However, the most popular and effective solution is the Tuned Mass Damper (TMD). Optimizing the parameters of this passive control system has attracted the attention of many researchers, leading to the study and development of numerous algorithms [12–14]. Recently, Djerouni et al. [15] determined the effectiveness of using the tuned mass damper inerter (TMDI) and the tuned inerter damper (TID) to mitigate seismic pounding.

The reduction of the vulnerability of a structure requires a good knowledge of the structure and the soil that supports it. The global term for the study of these phenomena is soil-structure interaction (SSI). Many researchers have been focusing on this issue. (See, for example, Mylonakis and Gazetas [16], Mekki et al. [17], Oz et al. [18], Arboleda-Monsalve et al. [19], Liu et al. [20] and Kaveh and Ardebili [21]). They concluded that not only does the nature of the soil influence the behavior of the structure, but also that the structure influences the behavior of the soil. Furthermore, the effects of SSI play an important role in determining the dynamic response of structures, and neglecting SSI can lead to unsafe construction, especially for structures built on soft ground.

The importance of considering SSI in pounding problems has been confirmed by several researchers (for example, Sobhi and Far [22]). Moreover, Mahmoud et al. [23] studied the impact of both the supporting soil flexibility and the pounding between adjacent structures. The findings of this study indicated that including SSI reduces the peak impact forces and story peak displacements during collisions while increasing the peak accelerations. However, Pawar and Murnal [24] concluded that taking SSI into account increases structural displacement while decreasing other reactions such as base shear, impact force, and kinetic energy. In addition, the phenomenon of SSI may produce severe pounding due to an increase in displacement. Therefore, neglecting SSI may lead to incorrect conclusions about the risk of pounding. The studies have also shown that SSI has considerably increased the effect of pounding on flexible buildings compared to stiffer structures when SSI is considered [25].

There is limited research about the effects of soil type on the dynamic response of adjacent buildings when considering SSI. Recently, Miari and Jankowski [26, 27] examined the impact of pounding between structures built on the same and various soil types (hard rock, rock, very dense soil, soft rock, stiff soil, and soft clay soil). The results showed that buildings constructed on soft clay soil are susceptible to the greatest displacements and shear forces, followed by structures built on stiff soil, then structures built on very dense soil and soft rock. Finally, structures built on rock and hard rock experienced the lowest displacement and shear forces. Tena-Colunga and Sánchez-Ballinas [28] conducted a parametric study to minimize heavy pounding on soft soils. They concluded that the seismic code of Mexico City should increase the minimum distance between neighboring structures.

Until now, the impact of pounding on the responses of colliding buildings considering Soil-Structure Interaction (SSI) has not been fully understood, and the results are

generally contradictory. Previous investigations were limited to comparing the responses of colliding buildings in cases with fixed bases and incorporating SSI. These studies focused on a single soil type and neglected the significance of uncertainty related to the soil, the parameters of the structure, or the seismic action. However, the vulnerability of adjacent structures might increase significantly due to the variability of these parameters. These variabilities are an important source of uncertainty. It is in this context that the objective of this paper is articulated. This study aims to determine the effect of different types of uncertainties (structural parameters, soil parameters, and seismic action) on the response of adjacent structures, considering the SSI.

To achieve the objectives of this article, two multistory buildings of equal height have been considered in the study. These buildings have been modeled as inelastic lumped mass systems, with the structure on the right being stiffer than the one on the left. The models have been excited using the time history of the El Centro earthquake (May 18, 1940). Additionally, the modified linear viscoelastic contact element was employed to simulate the pounding phenomenon, and the spring-dashpot elements have been incorporated to account for the dynamic behavior of the supporting soil.

2 Numerical models
2.1 Model of the adjacent structures and the SSI
The adjacent structures are typically modeled as multi-degree-of-freedom (MDOF) systems, with lumped masses concentrated at the levels of their floors. as shown in Fig. 2. Two 10-story buildings with different dynamic properties, where the masses, stiffnesses, and damping coefficients for the left building are represented by m_1^L, m_2^L, m_3^L,..., m_{10}^L; k_1^L, k_2^L, k_3^L,..., k_{10}^L; and C_1^L, C_2^L, C_3^L,..., C_{10}^L; respectively, whereas the masses, stiffnesses, and damping coefficients for the right building are represented by m_1^R, m_2^R, m_3^R,..., m_{10}^R; k_1^R, k_2^R, k_3^R,..., k_{10}^R; and C_1^R, C_2^R, C_3^R,..., C_{10}^R; respectively. The structures shown are separated by distances (d), see Fig. 2.

The theory of a homogeneous, isotropic, and elastic half-space has been used to consider the SSI. The translation and the rotation of the foundation are simulated using springs and dampers adapted to the horizontal and rotational movement of the supporting soil [29], see Fig. 3. The soil-foundation parameters are dependent on the elastic properties of the soil and the dimensions of the foundation.

These parameters consist of horizontal stiffness and damping (Eq. (1)) and rocking stiffness and damping (Eq. (2)) [29].
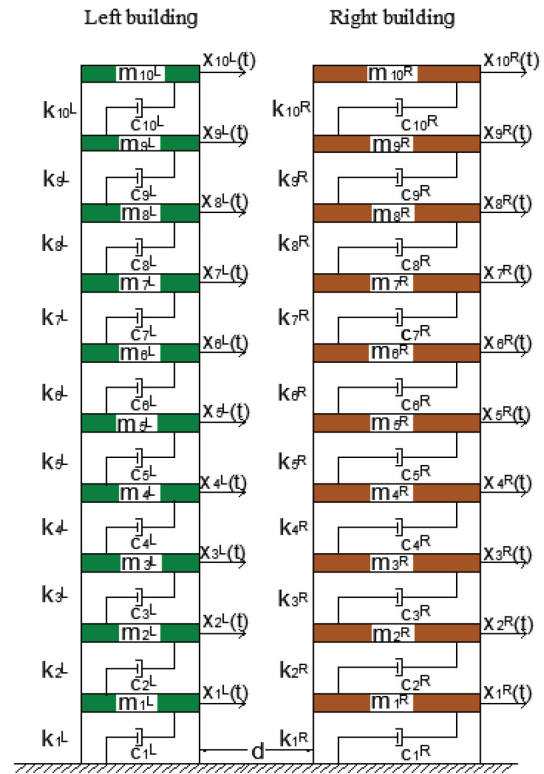
Fig. 2 Model of the two colliding buildings
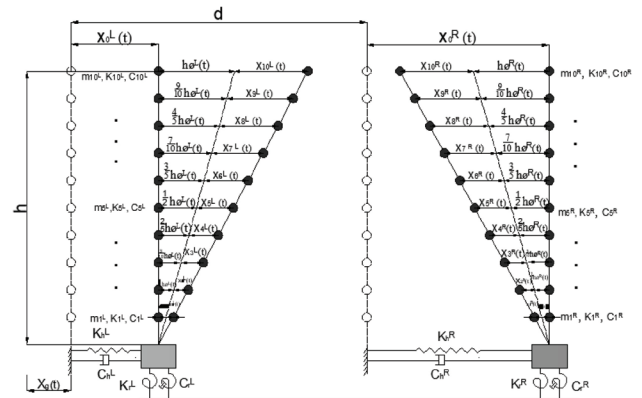
Fig. 3 Model of the two colliding buildings considering SSI

$$K_h = 2(1-v)G\beta_x\sqrt{BL}; C_h = 0.576K_h r_h\sqrt{\frac{\rho}{G}} \quad (1)$$

$$K_r = \frac{G}{1-v}\beta_\phi BL^2; C_r = \frac{0.3}{1+\beta_\phi}K_r r_r\sqrt{\frac{\rho}{G}} \quad (2)$$

Where the dimensions of the foundations are ($B \times L$), β_x and β_ϕ are the correct constants of sway and rocking spring. r_h and r_r are the equivalent radii of isolated foundations for sway and rocking springs. Whereas the soil properties are defined by Poisson's ratio v, the mass density ρ, and the maximum shear modulus G_{max}, which depends on the shear wave velocity V_s (Eq. (3)) [29].

$$G_{\max} = \rho(V_s)^2 \tag{3}$$

In the analysis that incorporates SSI, the shear modulus has been decreased to more accurately reflect the behavior of the soil. In this study, the reduced shear modulus G was assumed to be 50% of the maximum shear modulus $G_{\max}$ and calculated by (Eq. (3)) [29].

2.2 Model for simulating pounding force during collision

The linear viscoelastic model has been extensively and successfully used in the majority of studies on earthquake-induced structural pounding [8] because it is the most efficient and practical model to simulate the pounding force. Also, it takes into account the energy dissipation during the collision. However, the drawback of this model is the negative impact force observed just before the separation of colliding structures. To eliminate this default, Mahmoud and Jankowski [30] modified the linear viscoelastic model by activating the damping term only during the approach period of the collision.

In our case, we used the modified linear viscoelastic model (Fig. 4), which consists of three sub-elements. In the middle part, a linear spring accounts for pounding-induced elastic force, and a linear dashpot takes into account the energy dissipation during the collision. On the right, the separation gap is simulated by a GAP element. These impact elements are presented between the masses and activated only if the separation gap is closed, and the two masses are in contact. Otherwise, the impact force is transmitted to zero.

The pounding force during impact $F(t)$, for this model is defined by Eq. (4).
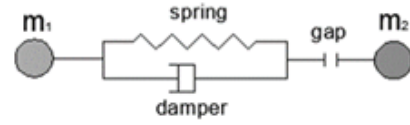

Fig. 4 Model of pounding force

$$F(t) = k\delta(t) + c\dot{\delta}(t) \text{ for } \dot{\delta}(t) > 0 \text{ (approach period)}$$
$$F(t) = k\delta(t) \text{ for } \dot{\delta}(t) \le 0 \text{ (restitution period)} \tag{4}$$

Where δ is the deformation of colliding structural elements, $\dot{\delta}$ is the relative velocity between colliding structural elements, k is the impact element's stiffness, and c is the impact element's damping, which can be defined by Eq. (5), see [8, 31].

$$c = 2\xi\sqrt{k\frac{m_1 m_2}{m_1 + m_2}} \tag{5}$$

Where m_1 and m_2 are the masses, as illustrated in Fig. 4. Moreover, the relation between the impact damping ratio ξ and the coefficient of restitution e is defined by Eq. (6) [30].

$$\xi = \frac{1-e^2}{e(e(\pi-2)+2)} \tag{6}$$

3 Dynamic equation of motions

The dynamic equation of motion for colliding buildings considering SSI, as shown in Fig. 3, is expressed by Eq. (7) [25].

$$\begin{bmatrix} M^L & 0 \\ 0 & M^R \end{bmatrix}\begin{pmatrix} \ddot{U}^L \\ \ddot{U}^R \end{pmatrix} + \begin{bmatrix} C^L & 0 \\ 0 & C^R \end{bmatrix}\begin{pmatrix} \dot{U}^L \\ \dot{U}^R \end{pmatrix} + \begin{bmatrix} R^L & 0 \\ 0 & R^R \end{bmatrix} + \begin{pmatrix} F \\ -F \end{pmatrix} =$$
$$-\begin{bmatrix} M^{*L} & 0 \\ 0 & M^{*R} \end{bmatrix}\begin{pmatrix} \ddot{U}_g \\ \ddot{U}_g \end{pmatrix} \tag{7}$$

$$\ddot{U}^L = \begin{pmatrix} \ddot{u}_1^L \\ \ddot{u}_2^L \\ \ddot{u}_3^L \\ \ddot{u}_4^L \\ \ddot{u}_5^L \\ \ddot{u}_6^L \\ \ddot{u}_7^L \\ \ddot{u}_8^L \\ \ddot{u}_9^L \\ \ddot{u}_{10}^L \\ \ddot{u}_0^L \\ \ddot{\phi}^L \end{pmatrix}; \ \dot{U}^L = \begin{pmatrix} \dot{u}_1^L \\ \dot{u}_2^L \\ \dot{u}_3^L \\ \dot{u}_4^L \\ \dot{u}_5^L \\ \dot{u}_6^L \\ \dot{u}_7^L \\ \dot{u}_8^L \\ \dot{u}_9^L \\ \dot{u}_{10}^L \\ \dot{u}_0^L \\ \dot{\phi}^L \end{pmatrix}; \ U^L = \begin{pmatrix} u_1^L \\ u_2^L \\ u_3^L \\ u_4^L \\ u_5^L \\ u_6^L \\ u_7^L \\ u_8^L \\ u_9^L \\ u_{10}^L \\ u_0^L \\ \phi^L \end{pmatrix}; \ \ddot{U}^R = \begin{pmatrix} \ddot{u}_1^R \\ \ddot{u}_2^R \\ \ddot{u}_3^R \\ \ddot{u}_4^R \\ \ddot{u}_5^R \\ \ddot{u}_6^R \\ \ddot{u}_7^R \\ \ddot{u}_8^R \\ \ddot{u}_9^R \\ \ddot{u}_{10}^R \\ \ddot{u}_0^R \\ \ddot{\phi}^R \end{pmatrix}; \ \dot{U}^R = \begin{pmatrix} \dot{u}_1^R \\ \dot{u}_2^R \\ \dot{u}_3^R \\ \dot{u}_4^R \\ \dot{u}_5^R \\ \dot{u}_6^R \\ \dot{u}_7^R \\ \dot{u}_8^R \\ \dot{u}_9^R \\ \dot{u}_{10}^R \\ \dot{u}_0^R \\ \dot{\phi}^R \end{pmatrix}; \ U^R = \begin{pmatrix} u_1^R \\ u_2^R \\ u_3^R \\ u_4^R \\ u_5^R \\ u_6^R \\ u_7^R \\ u_8^R \\ u_9^R \\ u_{10}^R \\ u_0^R \\ \phi^R \end{pmatrix} \tag{8}$$

$$M^L = \begin{bmatrix}
m_1^L & 0 & 0 & 0 & 0 & 0 & 0 & 0 & 0 & 0 & m_1^L & \left(m_1^L h/10\right) \\
0 & m_2^L & 0 & 0 & 0 & 0 & 0 & 0 & 0 & 0 & m_2^L & \left(m_2^L h/5\right) \\
0 & 0 & m_3^L & 0 & 0 & 0 & 0 & 0 & 0 & 0 & m_3^L & \left(3m_3^L h/10\right) \\
0 & 0 & 0 & m_4^L & 0 & 0 & 0 & 0 & 0 & 0 & m_4^L & \left(2m_4^L h/5\right) \\
0 & 0 & 0 & 0 & m_5^L & 0 & 0 & 0 & 0 & 0 & m_5^L & \left(m_5^L h/2\right) \\
0 & 0 & 0 & 0 & 0 & m_6^L & 0 & 0 & 0 & 0 & m_6^L & \left(3m_6^L h/5\right) \\
0 & 0 & 0 & 0 & 0 & 0 & m_7^L & 0 & 0 & 0 & m_7^L & \left(7m_7^L h/10\right) \\
0 & 0 & 0 & 0 & 0 & 0 & 0 & m_8^L & 0 & 0 & m_8^L & \left(4m_8^L h/5\right) \\
0 & 0 & 0 & 0 & 0 & 0 & 0 & 0 & m_9^L & 0 & m_9^L & \left(9m_9^L h/10\right) \\
0 & 0 & 0 & 0 & 0 & 0 & 0 & 0 & 0 & m_{10}^L & m_{10}^L & \left(m_{10}^L h\right) \\
m_1^L & m_2^L & m_3^L & m_4^L & m_5^L & m_6^L & m_7^L & m_8^L & m_9^L & m_{10}^L & \left(m_1^L+....+m_{10}^L\right) & h\left(\left(m_1^L/10\right)+\ldots+m_{10}^L\right) \\
\left(\dfrac{m_1^L h}{10}\right) & \left(\dfrac{m_2^L h}{5}\right) & \left(\dfrac{3m_3^L h}{10}\right) & \left(\dfrac{2m_4^L h}{5}\right) & \left(\dfrac{m_5^L h}{2}\right) & \left(\dfrac{3m_6^L h}{5}\right) & \left(\dfrac{7m_7^L h}{10}\right) & \left(\dfrac{4m_8^L h}{5}\right) & \left(\dfrac{9m_9^L h}{10}\right) & m_{10}^L h & h\left(\dfrac{m_1^L}{10}+\ldots+m_{10}^L\right) & h^2\left(\left(m_1^L/100\right)+\ldots+m_{10}^L\right)
\end{bmatrix} \tag{9}$$

$$M^R = \begin{bmatrix}
m_1^R & 0 & 0 & 0 & 0 & 0 & 0 & 0 & 0 & 0 & m_1^R & \left(m_1^R h/10\right) \\
0 & m_2^R & 0 & 0 & 0 & 0 & 0 & 0 & 0 & 0 & m_2^R & \left(m_2^R h/5\right) \\
0 & 0 & m_3^R & 0 & 0 & 0 & 0 & 0 & 0 & 0 & m_3^R & \left(3m_3^R h/10\right) \\
0 & 0 & 0 & m_4^R & 0 & 0 & 0 & 0 & 0 & 0 & m_4^R & \left(2m_4^R h/5\right) \\
0 & 0 & 0 & 0 & m_5^R & 0 & 0 & 0 & 0 & 0 & m_5^R & \left(m_5^R h/2\right) \\
0 & 0 & 0 & 0 & 0 & m_6^R & 0 & 0 & 0 & 0 & m_6^R & \left(3m_6^R h/5\right) \\
0 & 0 & 0 & 0 & 0 & 0 & m_7^R & 0 & 0 & 0 & m_7^R & \left(7m_7^R h/10\right) \\
0 & 0 & 0 & 0 & 0 & 0 & 0 & m_8^R & 0 & 0 & m_8^R & \left(4m_8^R h/5\right) \\
0 & 0 & 0 & 0 & 0 & 0 & 0 & 0 & m_9^R & 0 & m_9^R & \left(9m_9^R h/10\right) \\
0 & 0 & 0 & 0 & 0 & 0 & 0 & 0 & 0 & m_{10}^R & m_{10}^R & \left(m_{10}^R h\right) \\
m_1^R & m_2^R & m_3^R & m_4^R & m_5^R & m_6^R & m_7^R & m_8^R & m_9^R & m_{10}^R & \left(m_1^R+....+m_{10}^R\right) & h\left(\left(m_1^R/10\right)+\ldots+m_{10}^R\right) \\
\left(\dfrac{m_1^R h}{10}\right) & \left(\dfrac{m_2^R h}{5}\right) & \left(\dfrac{3m_3^R h}{10}\right) & \left(\dfrac{2m_4^R h}{5}\right) & \left(\dfrac{m_5^R h}{2}\right) & \left(\dfrac{3m_6^R h}{5}\right) & \left(\dfrac{7m_7^R h}{10}\right) & \left(\dfrac{4m_8^R h}{5}\right) & \left(\dfrac{9m_9^R h}{10}\right) & m_{10}^R h & h\left(\dfrac{m_1^R}{10}+\ldots+m_{10}^R\right) & h^2\left(\left(m_1^R/100\right)+\ldots+m_{10}^R\right)
\end{bmatrix} \tag{10}$$

$$C^L = \begin{bmatrix}
\left(c_1^L+c_2^L\right) & -c_2^L & 0 & 0 & 0 & 0 & 0 & 0 & 0 & 0 & 0 & 0 \\
-c_2^L & \left(c_2^L+c_3^L\right) & -c_3^L & 0 & 0 & 0 & 0 & 0 & 0 & 0 & 0 & 0 \\
0 & -c_3^L & \left(c_3^L+c_4^L\right) & -c_4^L & 0 & 0 & 0 & 0 & 0 & 0 & 0 & 0 \\
0 & 0 & -c_4^L & \left(c_4^L+c_5^L\right) & -c_5^L & 0 & 0 & 0 & 0 & 0 & 0 & 0 \\
0 & 0 & 0 & -c_5^L & \left(c_5^L+c_6^L\right) & -c_6^L & 0 & 0 & 0 & 0 & 0 & 0 \\
0 & 0 & 0 & 0 & -c_6^L & \left(c_6^L+c_7^L\right) & -c_7^L & 0 & 0 & 0 & 0 & 0 \\
0 & 0 & 0 & 0 & 0 & -c_7^L & \left(c_7^L+c_8^L\right) & -c_8^L & 0 & 0 & 0 & 0 \\
0 & 0 & 0 & 0 & 0 & 0 & -c_8^L & \left(c_8^L+c_9^L\right) & -c_9^L & 0 & 0 & 0 \\
0 & 0 & 0 & 0 & 0 & 0 & 0 & -c_9^L & \left(c_9^L+c_{10}^L\right) & -c_{10}^L & 0 & 0 \\
0 & 0 & 0 & 0 & 0 & 0 & 0 & 0 & -c_{10}^L & c_{10}^L & 0 & 0 \\
0 & 0 & 0 & 0 & 0 & 0 & 0 & 0 & 0 & 0 & C_h^L & 0 \\
0 & 0 & 0 & 0 & 0 & 0 & 0 & 0 & 0 & 0 & 0 & C_r^L
\end{bmatrix} \tag{11}$$

$$C^R = \begin{bmatrix} (c_1^R + c_2^R) & -c_2^R & 0 & 0 & 0 & 0 & 0 & 0 & 0 & 0 & 0 & 0 \\ -c_2^R & (c_2^R + c_3^R) & -c_3^R & 0 & 0 & 0 & 0 & 0 & 0 & 0 & 0 & 0 \\ 0 & -c_3^R & (c_3^R + c_4^R) & -c_4^R & 0 & 0 & 0 & 0 & 0 & 0 & 0 & 0 \\ 0 & 0 & -c_4^R & (c_4^R + c_5^R) & -c_5^R & 0 & 0 & 0 & 0 & 0 & 0 & 0 \\ 0 & 0 & 0 & -c_5^R & (c_5^R + c_6^R) & -c_6^R & 0 & 0 & 0 & 0 & 0 & 0 \\ 0 & 0 & 0 & 0 & -c_6^R & (c_6^R + c_7^R) & -c_7^R & 0 & 0 & 0 & 0 & 0 \\ 0 & 0 & 0 & 0 & 0 & -c_7^R & (c_7^R + c_8^R) & -c_8^R & 0 & 0 & 0 & 0 \\ 0 & 0 & 0 & 0 & 0 & 0 & -c_8^R & (c_8^R + c_9^R) & -c_9^R & 0 & 0 & 0 \\ 0 & 0 & 0 & 0 & 0 & 0 & 0 & -c_9^R & (c_9^R + c_{10}^R) & -c_{10}^R & 0 & 0 \\ 0 & 0 & 0 & 0 & 0 & 0 & 0 & 0 & -c_{10}^R & c_{10}^R & 0 & 0 \\ 0 & 0 & 0 & 0 & 0 & 0 & 0 & 0 & 0 & 0 & C_h^R & 0 \\ 0 & 0 & 0 & 0 & 0 & 0 & 0 & 0 & 0 & 0 & 0 & C_r^R \end{bmatrix} \tag{12}$$

$$R^L = \begin{pmatrix} R_1^L - R_2^L \\ R_2^L - R_3^L \\ R_3^L - R_4^L \\ R_4^L - R_5^L \\ R_5^L - R_6^L \\ R_6^L - R_7^L \\ R_7^L - R_8^L \\ R_8^L - R_9^L \\ R_9^L - R_{10}^L \\ R_{10}^L \\ K_h^L u_0^L \\ K_r^L \phi^L \end{pmatrix}; \quad R^R = \begin{pmatrix} R_1^R - R_2^R \\ R_2^R - R_3^R \\ R_3^R - R_4^R \\ R_4^R - R_5^R \\ R_5^R - R_6^R \\ R_6^R - R_7^R \\ R_7^R - R_8^R \\ R_8^R - R_9^R \\ R_9^R - R_{10}^R \\ R_{10}^R \\ K_h^R u_0^R \\ K_r^R \phi^R \end{pmatrix}; \quad F = \begin{pmatrix} F_{11} \\ F_{22} \\ F_{33} \\ F_{44} \\ F_{55} \\ F_{66} \\ F_{77} \\ F_{88} \\ F_{99} \\ F_{1010} \\ 0 \\ 0 \end{pmatrix}; \quad \ddot{U}_g = \begin{pmatrix} \ddot{u}_g \\ \ddot{u}_g \\ \ddot{u}_g \\ \ddot{u}_g \\ \ddot{u}_g \\ \ddot{u}_g \\ \ddot{u}_g \\ \ddot{u}_g \\ \ddot{u}_g \\ \ddot{u}_g \\ \ddot{u}_g \\ \ddot{u}_g \end{pmatrix} \tag{13}$$

$$M^{*L} = \begin{bmatrix} m_1^L & 0 & 0 & 0 & 0 & 0 & 0 & 0 & 0 & 0 & 0 & 0 \\ 0 & m_2^L & 0 & 0 & 0 & 0 & 0 & 0 & 0 & 0 & 0 & 0 \\ 0 & 0 & m_3^L & 0 & 0 & 0 & 0 & 0 & 0 & 0 & 0 & 0 \\ 0 & 0 & 0 & m_4^L & 0 & 0 & 0 & 0 & 0 & 0 & 0 & 0 \\ 0 & 0 & 0 & 0 & m_5^L & 0 & 0 & 0 & 0 & 0 & 0 & 0 \\ 0 & 0 & 0 & 0 & 0 & m_6^L & 0 & 0 & 0 & 0 & 0 & 0 \\ 0 & 0 & 0 & 0 & 0 & 0 & m_7^L & 0 & 0 & 0 & 0 & 0 \\ 0 & 0 & 0 & 0 & 0 & 0 & 0 & m_8^L & 0 & 0 & 0 & 0 \\ 0 & 0 & 0 & 0 & 0 & 0 & 0 & 0 & m_9^L & 0 & 0 & 0 \\ 0 & 0 & 0 & 0 & 0 & 0 & 0 & 0 & 0 & m_{10}^L & 0 & 0 \\ 0 & 0 & 0 & 0 & 0 & 0 & 0 & 0 & 0 & 0 & (m_1^L + \ldots + m_{10}^L) & 0 \\ 0 & 0 & 0 & 0 & 0 & 0 & 0 & 0 & 0 & 0 & 0 & h\left(\dfrac{m_1^L}{10} + \ldots + m_{10}^L\right) \end{bmatrix} \tag{14}$$

$$M^{*R} = \begin{bmatrix} m_1^R & 0 & 0 & 0 & 0 & 0 & 0 & 0 & 0 & 0 & 0 & 0 \\ 0 & m_2^R & 0 & 0 & 0 & 0 & 0 & 0 & 0 & 0 & 0 & 0 \\ 0 & 0 & m_3^R & 0 & 0 & 0 & 0 & 0 & 0 & 0 & 0 & \mathbf{0} \\ 0 & 0 & 0 & m_4^R & 0 & 0 & 0 & 0 & 0 & 0 & 0 & 0 \\ 0 & 0 & 0 & 0 & m_5^R & 0 & 0 & 0 & 0 & 0 & 0 & 0 \\ 0 & 0 & 0 & 0 & 0 & m_6^R & 0 & 0 & 0 & 0 & 0 & 0 \\ 0 & 0 & 0 & 0 & 0 & 0 & m_7^R & 0 & 0 & 0 & 0 & 0 \\ 0 & 0 & 0 & 0 & 0 & 0 & 0 & m_8^R & 0 & 0 & 0 & 0 \\ 0 & 0 & 0 & 0 & 0 & 0 & 0 & 0 & m_9^R & 0 & 0 & 0 \\ 0 & 0 & 0 & 0 & 0 & 0 & 0 & 0 & 0 & m_{10}^R & 0 & 0 \\ 0 & 0 & 0 & 0 & 0 & 0 & 0 & 0 & 0 & 0 & \left(m_1^R + \dots + m_{10}^R\right) & 0 \\ 0 & 0 & 0 & 0 & 0 & 0 & 0 & 0 & 0 & 0 & 0 & h\left(\dfrac{m_1^R}{10} + \dots + m_{10}^R\right) \end{bmatrix} \qquad (15)$$

Where ($\ddot{U}^L$, $\dot{U}^L$, U^L) and ($\ddot{U}^R$, $\dot{U}^R$, U^R) denote the acceleration, velocity, and displacement vectors for the left and the right buildings (Eq. (8)). M^L and M^R are the matrices of masses for the left and the right building (Eqs. (9) and (10)); C^L and C^R are the matrices of damping coefficients for the left and the right building (Eqs. (11) and (12)). R^L and R^R are the vectors consisting of the system resisting forces for the left and the right buildings (Eq. (13)). F is the pounding force vector, and $\ddot{U}_g$ is the vector of ground motion acceleration (Eq. (13)).

4 Case study

4.1 Description of the selected structures

The case study involves two 10-story adjacent structures with different dynamic characteristics, where the right structure is stiffer than the left structure. The plan and elevation views are illustrated in Figs. 5 (a) and 5 (b). The buildings are constructed using concrete, which has a strength of 25 MPa and Young's modulus of 32164.20 MPa.

The steel used has a yield strength of 400 MPa and a modulus of elasticity of 200 GPa. The structures were designed as a column-beam system, and the columns are square with a dimension of (50×50) m^2 for the left structure and (60×60) m^2 for the right structure (Fig. 5(c)). The foundation has dimensions $B = L = 2.50$ m for both structures, see Fig. 5(c). The floors are infinitely rigid, with a live load $Q = 1.5$ KN/m^2 and a roof load $G = 5.14$ KN/m^2.

4.2 Variability

The soil is a heterogeneous material since it consists of several layers whose properties are constantly changing due to soil disaggregation, which induces the variability of soil properties from one area to another. That is known as the natural variability or spatial variability of the soil.

This topic has been investigated in numerous studies [32, 33]. Also, the effect of uncertainty on the structural response has been extensively discussed [34–37], considering that it can provide more reliable results and allow for more precise construction of the structures given that the material properties and geometric elements of a building are uncertain due to various reasons. Despite all that, the impact of uncertainty on the behavior of colliding buildings has received limited attention. For an effective investigation, it's crucial to consider all sources of variability, which are significant sources of uncertainty.

A detailed analysis of the seismic behavior of adjacent structures requires the control and consideration of several types of uncertainties:

- Structural uncertainty: the variability of structural geometry on the one hand and the variability of material characteristics (strength, Young's modulus, etc.) on the other.
- Soil uncertainty: characterization of mechanical properties (spatial variability) due to soil heterogeneity.
- Uncertainty related to seismic action: Earthquakes differ inherently due to their nature, unpredictability, intensity, frequency content, and type of seismogenic source.
- Soil-structure interaction uncertainty: modeling impedance functions and soil-foundation liaison.

To reach the target of this study, all uncertainties resulting from the variation of structural parameters, soil parameters, and seismic action have been included. Seven variables have been considered: the building's mass coefficient (m), the building's stiffness coefficient (k), the building's damping factor (c), the Poisson's ratio of the soil, the density of the soil (ρ), soil shear wave velocity (V_s),

Left structure

Right structure

(a)

(b)

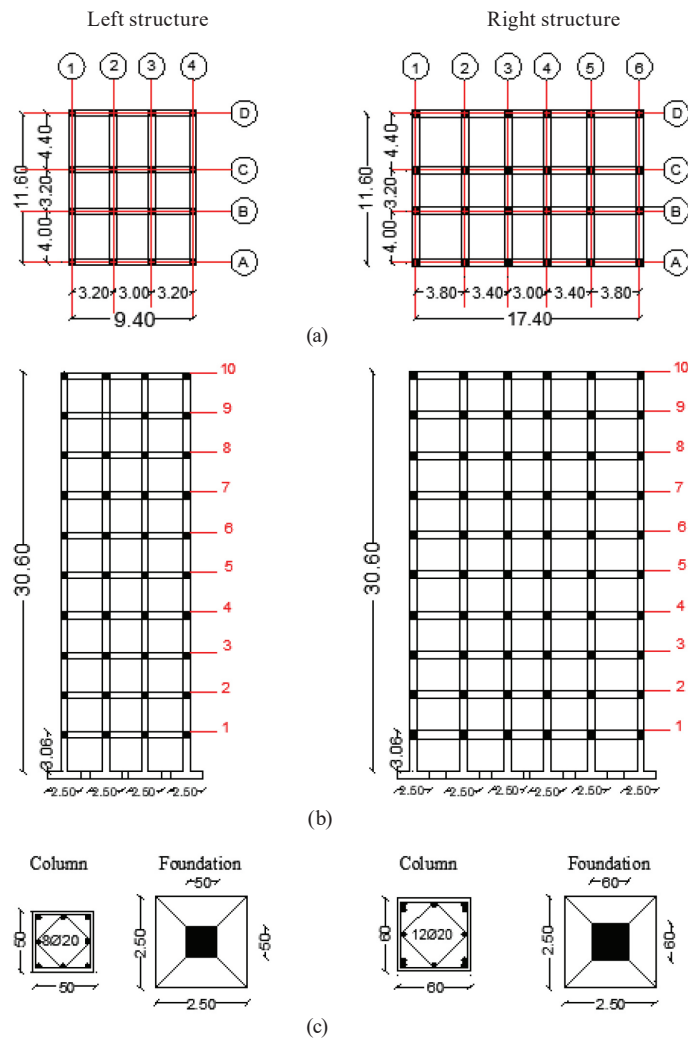Column Foundation Column Foundation

(c)

Fig. 5 Description of the selected structure; (a) Plan view, (b) Elevation view, (c) Geometric characteristics for column and foundation

and peak ground acceleration (PGA). Each one of these parameters has been described by probability distribution laws defined by their mean and coefficients of variation (CoV), or their mean and their minimum and maximum values as indicated in Table 1.

5 Numerical results

Numerical simulations based on the Matlab code were used to evaluate the seismic behavior of colliding buildings, including the soil-structure interaction and the variability of structural parameters, soil parameters, and seismic action.

The model has been excited using the time history of the El Centro earthquake (May 18, 1940). To account for both horizontal and rotational movements of the supporting soil, swaying, rocking springs, and dashpots have been employed, see Fig. 3. The horizontal and rotational stiffness and damping coefficients have been calculated using the formulas given by Eqs. (1) and (2). The corrected constants

of swaying and rocking springs have been taken as $\beta_x = 1$, $\beta_\phi = 0.5$. The radii of equivalent circular foundations for swaying and rocking springs have been estimated and found to be equal to $r_r = 1.41$ m and $r_h = 1.42$ m. The adjacent structures have been modeled as MDOF systems with lumped masses at the floor levels, see Fig. 2, and the separation gap distance has been considered as $d = 3$ cm.

The pounding force has been modeled using the modified linear viscoelastic model (Fig. 4). The stiffness of the spring has been taken to be equal to $k = 2.36 \times 10^7$ N/m, while the impact element's damping has been calculated based on Eq. (5) for the coefficient of restitution $e = 0.65$ [38]. The analysis has been performed in two cases: deterministic analysis and probabilistic analysis.

5.1 Results of the deterministic analysis

The mean values of the different parameters have been selected for deterministic analysis (see Table 1). In addition, four soil types with different shear wave velocities have

Table 1 The probabilistic properties of variables

Variable	Uncertainty parameters		Distribution	Mean	CoV	Minimum value	Maximum value
Structural parameters	m^L (kg)		Log-normal	53164.903	0.10	-	-
	m^R (kg)		Log-normal	104643.441	0.10	-	-
	k^L (N/m)		Log-normal	5.613×10^8	0.10	-	-
	k^R (N/m)		Log-normal	1.746×10^9	0.10	-	-
	c^L (kg/s)		Log-normal	1.123×10^6	0.10	-	-
	c^R (kg/s)		Log-normal	3.492×10^6	0.10	-	-
	ρ (kg/m³)		Uniform	1.81×10^3	-	1.7×10^3	1.9×10^3
	v		Uniform	0.29	-	0.25	0.33
Soil parameters	V_s (m/s)	Very soft soil	Uniform	125	-	50	200
		Soft soil	Uniform	300	-	200	400
		Hard soil	Uniform	600	-	400	800
		Rocky soil	Uniform	1350	-	800	1900
Seismic load	PGA (g)		Uniform	0.4	-	0.01	1

been considered to account for soil variability: $V_s = 125$ m/s, $V_s = 300$ m/s, $V_s = 600$ m/s, and $V_s = 1350$ m/s. The effect of the variability of the soil on the behavior of colliding buildings has been discussed in this analysis.

Fig. 6 shows the peak story displacement at different floor levels of the left and right buildings under different soil types. The results presented in this figure have indicated that the highest peak displacements (0.21 m for the left structure and 0.20 m for the right structure) are obtained at the top floor level (10th story), whereas the lowest peak story displacements are obtained at the 1st story of the structures for both neighboring buildings.

The influence of the soil type has also been investigated at this stage. It has been shown that the buildings have significantly different structural responses under different site conditions. It can be seen from Fig. 6 that the peak displacement of the colliding buildings decreased with the increase in the soil shear wave velocity at all floor levels of the structures. Notably, buildings founded under the soil shear wave velocity of $V_s = 125$ m/s produced the highest levels of displacement, followed by those of $V_s = 300$ m/s, $V_s = 600$ m/s, and finally $V_s = 1350$ m/s.

An example of displacement time histories for the left and right structures at the 10th story under four different soil types is shown in Fig. 7. It can be seen from Figs. 6 and 7 that the displacements of the left building (0.21 m) and the displacements of the right building (0.20 m) are relatively similar when constructed on very soft soil, see Fig. 7(a). However, the results shown in Fig. 7(d) clearly demonstrate that the displacement of the left building (0.05 m) is greater than that of the right building (0.01 m) when they are constructed on rocky soil. In this case, the

left building undergoes a large displacement resulting from structural pounding due to its lighter weight and greater flexibility. On the other hand, the right building, being stiffer, is less affected by such displacements.

Fig. 8 shows the pounding force time histories for the two colliding buildings under different soil types at the 1st story, the 5th story, and the top floor. The results presented
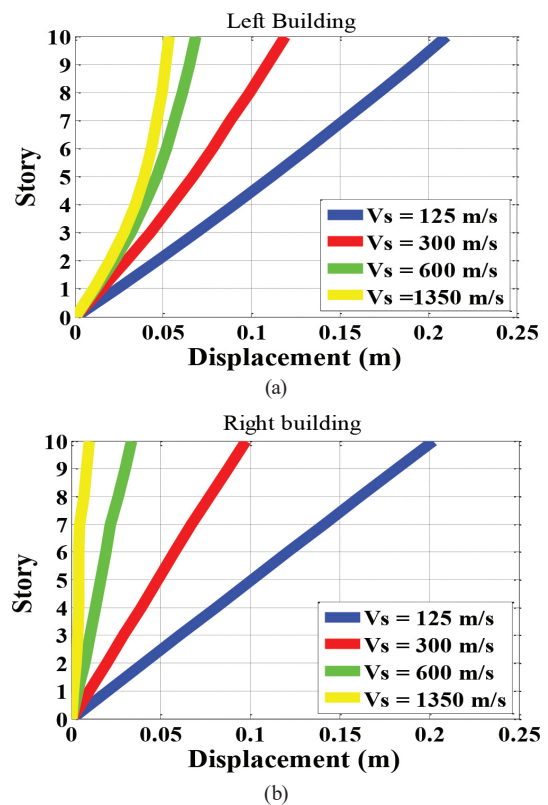

(a)

(b)

Fig. 6 Peak story displacement at different floor levels of the left and right buildings under different soil types; (a) left structure, (b) right structure
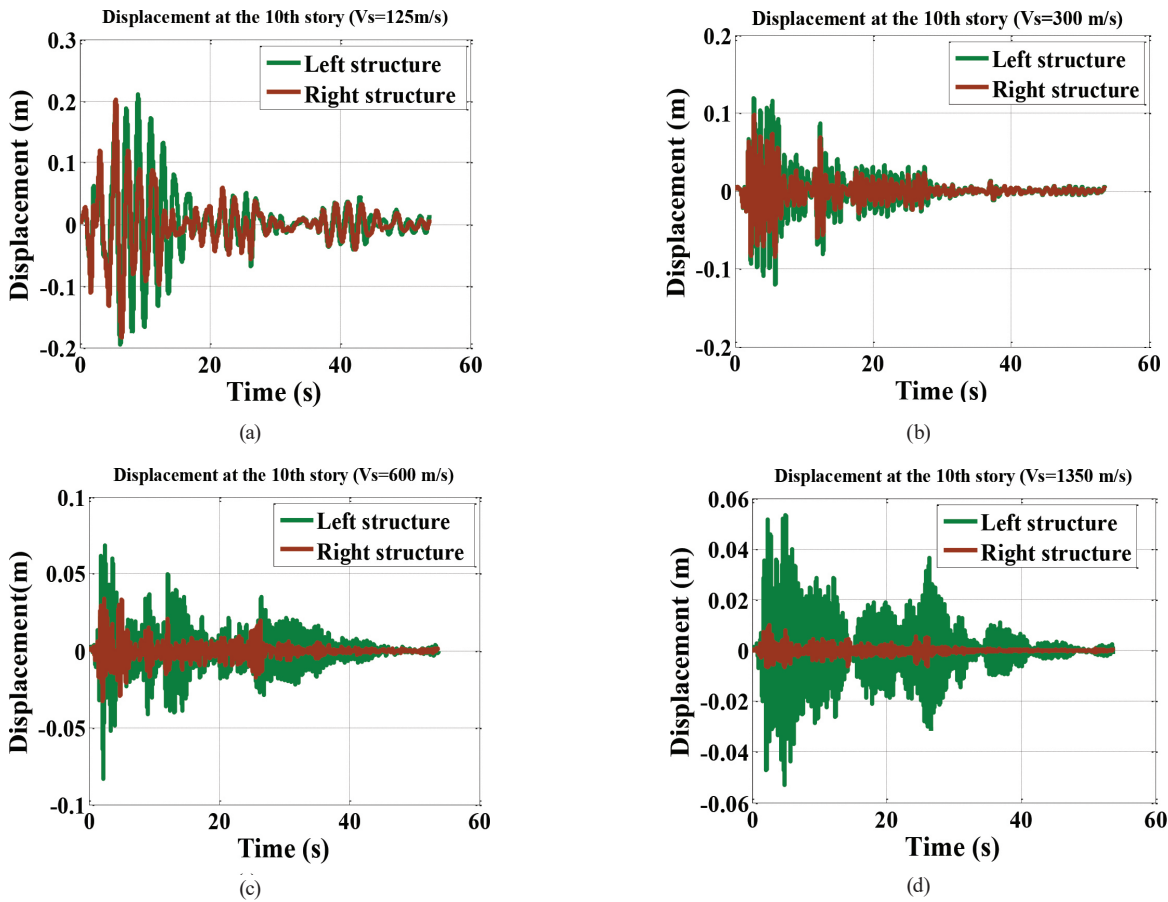
Fig. 7 Displacement time histories for the left and right buildings under different soil types; (a) $V_s = 125$ m/s, (b) $V_s = 300$ m/s, (c) $V_s = 600$ m/s, (d) $V_s = 1350$ m/s
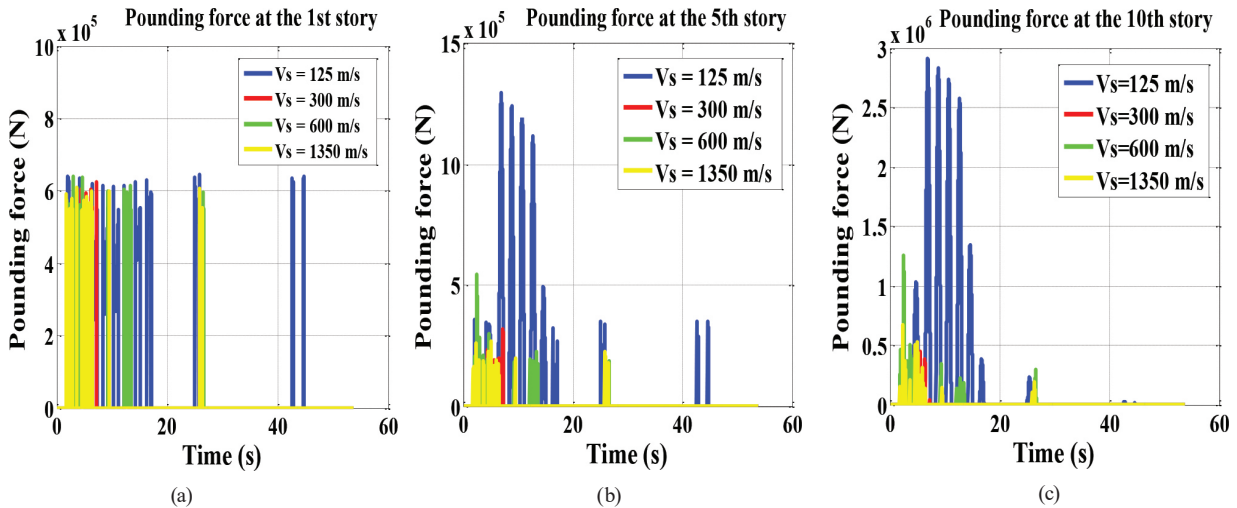

Fig. 8 Pounding time histories for the colliding buildings under different soil types; (a) at the 1st story, (b) at the 5th story, (c) at the 10th story

in this figure indicate that the highest pounding force is obtained at the top floor level, while the lowest pounding force is observed at the 1st story. For example, for buildings built under very soft soil ($V_s = 125$ m/s), the pounding force at the top floor is 2.92×10^6 N, while at the 1st floor, it is 6.44×10^5 N, see Fig. 8(c).

The influence of the soil type was also investigated at this stage, and the results have indicated that the buildings have significantly different structural responses under different site conditions. It can be seen from Fig. 8 that the pounding force of the colliding buildings decreased with the increase in the soil shear wave velocity at all floor

levels of the structures. Buildings founded under soil shear wave velocity $V_s = 125$ m/s produced the highest pounding force, followed by $V_s = 300$ m/s, $V_s = 600$ m/s, and finally $V_s = 1350$ m/s. That signifies that the very soft soil is the most affected by the collision.

5.2 Results of the probabilistic analysis

The probabilistic analysis has been considered with probabilistic parameters following the distribution laws defined by their mean and coefficients of variation (CoV), or their mean, minimum, and maximum values, as shown in Table 1. Moreover, 10,000 simulations have been performed to establish the probability curves (Figs. 8 and 9). The effect of the variability of structural parameters, soil parameters, and seismic action on the behavior of colliding buildings has been discussed in this analysis.

Fig. 9 compares the influence of the variability of structural parameters, soil parameters, and seismic action on the displacement probability of the two colliding buildings under different soil types at the 1st story, the 5th story, and the 10th story. The results presented in this figure have indicated that the probability of displacement at the level of the top floor (0.4 m) is higher than that of the other floors, whereas the lowest probabilities of displacement have been observed on the first story of both adjacent buildings.

The effect of soil type has also been studied at this stage. The results show that the dynamic responses of colliding buildings are significantly different for structures built on different soil types. Buildings built on very soft soil have the highest displacement probabilities, followed by those built on soft soil, hard soil, and rocky soil, in that order.
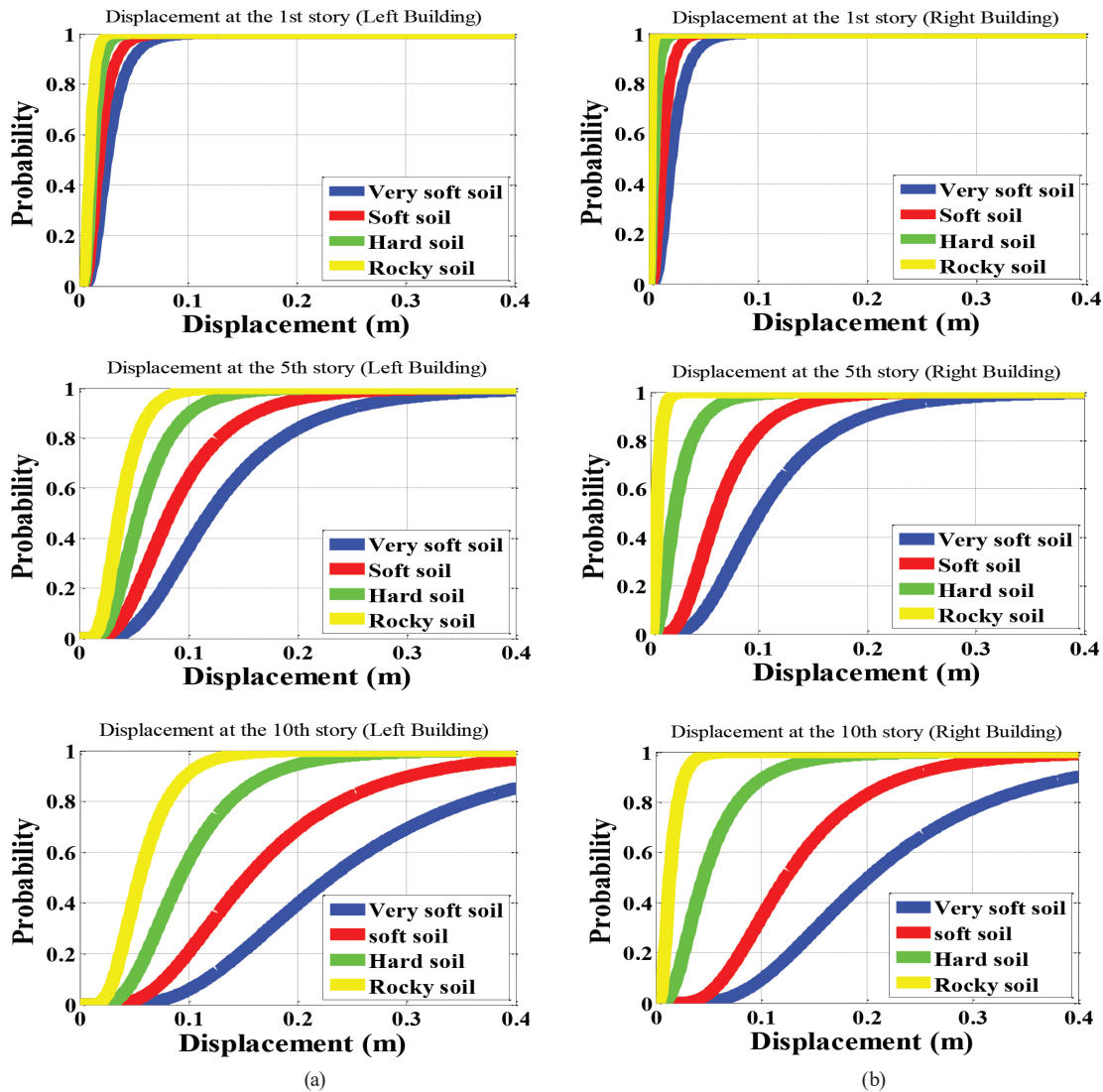

(a)   (b)

Fig. 9 The displacement probability of the two colliding buildings under different types of soil at the 1st story, the 5th story, and the 10th story; (a) Left building, (b) Right building

The comparison between Figs. 9(a) and 9(b) shows that the left building, which is lighter and more flexible, is more susceptible to undergoing higher displacement probabilities compared to the right building, which is stiffer. That is very clear for buildings constructed on rocky soil, where the displacement probability at the 10th story is 0.13 m for the left building and 0.04 m for the right building.
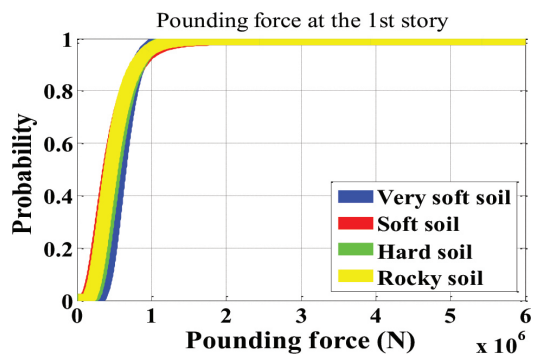
Fig. 10 compares the influence of the variability of structural parameters, soil parameters, and seismic action on the probability of pounding force under different soil types at the 1st story, the 5th story, and the top story. The results show that the top floor has a higher probability of pounding force (6×10^6 N) than the other floors, while the 1st story

(a)

(b)

(c)

Fig. 10 Probability of the pounding force between colliding buildings under different soil types; (a) at the 1st story, (b) at the 5th story, (c) at the 10th story

has the lowest probability of pounding force. The results shown in these figures show that the dynamic responses of colliding buildings are significantly different for structures built on different soil types.
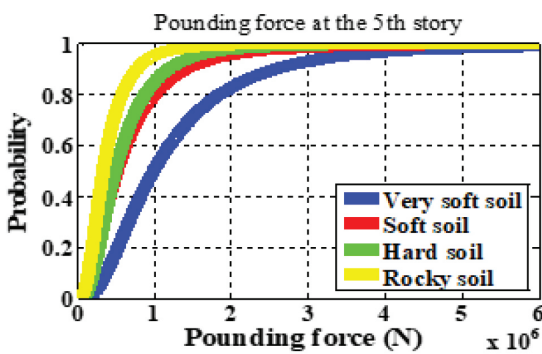
The highest pounding probabilities has been obtained for buildings built on very soft soil, then for buildings built on soft soil, then for buildings built on hard soil, and finally for buildings built on rocky soil, see Fig. 10.

The comparison between the results obtained from the deterministic analysis (Figs. 6, 7, and 8) and the probabilistic analysis (Figs. 9 and 10) has indicated that the probabilistic analysis provides more accurate results since it takes into account different types of uncertainties such as structural parameters, soil parameters, and seismic action. In contrast, deterministic analyses tend to underestimate the results by about 50 %, see Table 2.
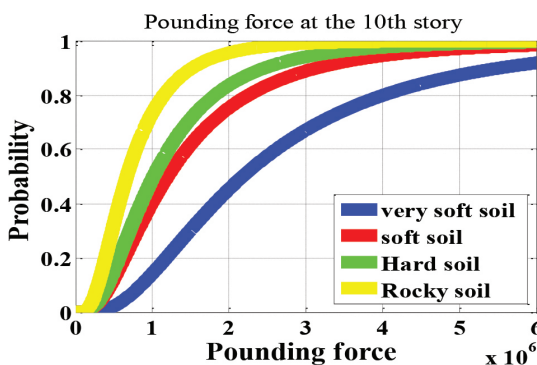
The analyses agree on the observation that the top floor experienced the highest level of impact during the collision. Moreover, the 1st floor is less affected by structural pounding when $d = 3$ cm, and the soil type significantly influences the dynamic responses during collisions. Additionally, the lighter structure is more susceptible to the effects of structural pounding.

6 Conclusions

This paper investigates the effect of the variability of structural parameters, soil parameters, and seismic action on the responses of two colliding buildings of the same height with different structural characteristics, taking into account SSI. The study is conducted in two cases: probabilistic analysis and deterministic analysis. First, the deterministic analysis is considered with deterministic parameters, and only the mean values of different parameters are accounted for. Then, the probabilistic analysis is performed with probabilistic parameters following the distribution laws defined by their mean and coefficients of variation (CoV), or their mean, minimum, and maximum values. Both analyses lead to the same conclusions.

Table 2 The important results of the two analyses for very soft soil

		Deterministic analysis	Probabilistic analysis
Displacement of the left building (m)	1st story	0.03	0.06
	10th story	0.21	0.40
Displacement of the right building (m)	1st story	0.02	0.05
	10th story	0.20	0.40
Pounding force (N)	1st story	6.44×10^5	10^6
	10th story	2.92×10^6	6×10^6

However, the probabilistic analysis provides a more precise estimation of the behavior of colliding buildings than the deterministic analysis.

The most important results of this work are as follows:
- The dynamic responses of the adjacent structures are higher at the top level, which indicates that the top floor is the most affected by the structural pounding.
- The soil type considerably affects the behavior of colliding buildings. It has been observed that an increase in the soil shear wave velocity reduced structural responses. Also, pounding is more severe in buildings built on very soft soil, followed by those on soft soil, hard soil, and rocky soil.

- Constructing on very soft soil is a highly challenging task that requires careful and detailed study.
- The behavior of each building, when subjected to structural pounding, is significantly influenced by the structural characteristics of adjacent buildings, including masses, stiffness, and damping factors.
- The study of the seismic behavior of colliding buildings requires a good knowledge of the structural parameters, the soil parameters, and the seismic action. However, neglecting the variability of these parameters may underestimate the structural responses, which may lead to erroneous results.

References

[1] Jankowski, R. "Non-linear FEM analysis of earthquake-induced pounding between the main building and the stairway tower of the Olive View Hospital", Engineering Structures, 31(8), pp. 1851–1864, 2009.
https://doi.org/10.1016/j.engstruct.2009.03.024

[2] Aguilar, J., Juarez, H., Ortega, R., Iglesias, J. " The Mexico Earthquake of September 19, 1985—Statistics of damage and of retrofitting techniques in reinforced concrete buildings affected by the 1985 earthquake ", Earthquake Spectra, 5(1), pp. 145–151, 1989.
https://doi.org/10.1193/1.1585516

[3] Kasai, K., Maison, B. F. "Building pounding damage during the 1989 Loma Prieta earthquake", Engineering Structures 19(3), pp. 195–207, 1996.
https://doi.org/10.1016/S0141-0296(96)00082-X

[4] Jain, S. K., Murty, C. V. R., Dayal, U., Jaswant, N. A., Sailender, K. C. "Learning from earthquakes: A field report on structural and geotechnical damages sustained during the 26 January 2001 M7. 9 Bhuj Earthquake in Western India", Department of Civil Engineering, Indian Institute of Technology, Kanpur, India, 2001.

[5] Cole, G. L., Dhakal, R. P., Turner, F. M. "Building pounding damage observed in the 2011 Christchurch earthquake", Earthquake Engineering & Structural Dynamics, 41(5), pp. 893–913, 2012.
https://doi.org/10.1002/eqe.1164

[6] Sharma, K., Deng, L., Noguez, C. C. "Field investigation on the performance of building structures during the April 25, 2015, Gorkha earthquake in Nepal", Engineering Structures, 121, pp. 61–74, 2016.
https://doi.org/10.1016/j.engstruct.2016.04.043

[7] Bechtoula, H., Ousalem, H. "The 21 May 2003 Zemmouri (Algeria) Earthquake: damages and disaster responses", Journal of Advanced Concrete Technology, 3(1), pp. 161–174, 2005.
https://doi.org/10.3151/jact.3.161

[8] Anagnostopoulos, S. A. "Pounding of buildings in series during earthquakes", Earthquake Engineering and Structural Dynamics, 16(3), pp. 443–456, 1988.
https://doi.org/10.1002/eqe.4290160311

[9] Jankowski, R. "Pounding force response spectrum under earthquake excitation", Engineering Structures, 28(8), pp. 1149–1161, 2006.
https://doi.org/10.1016/j.engstruct.2005.12.005

[10] Jankowski, R. "Earthquake-induced pounding between equal height buildings with substantially different dynamic properties", Engineering Structures, 30(10), pp. 2818–2829, 2008.
https://doi.org/10.1016/j.engstruct.2008.03.006

[11] Naserkhaki, S., Ghorbani, S. D., Tolloei, D. T. "Heavier adjacent building pounding due to earthquake excitation", [pdf] Asian Journal of Civil Engineering (BHRC), 14(2), pp. 349–367, 2013. Available at: https://www.sid.ir/EN/VEWSSID/J_pdf/103820130211.pdf

[12] Kaveh, A., Mohammadi, S., Hosseini, O. K., Keyhani, A., Kalatjari, V. R. "Optimum parameters of tuned mass dampers for seismic applications using charged system search", Iranian Journal of Science and Technology, Transactions of Civil Engineering, 39(C1), pp. 21–40, 2015.
https://doi.org/10.22099/IJSTC.2015.2739

[13] Kaveh, A., Pirgholizadeh, S., Khadem, H. O. "Semi-active tuned mass damper performance with optimized fuzzy controller using CSS algorithm", [pdf] Asian Journal of Civil Engineering, 16(5), pp. 587–606, 2015. Available at: https://www.sid.ir/en/VEWSSID/J_pdf/103820150502.pdf

[14] Kaveh, A., Farzam, M. F., Maroofiazar, R. "Comparing H2 and H∞ algorithms for optimum design of tuned mass dampers under near-fault and far-fault earthquake motions", Periodica Polytechnica Civil Engineering, 64(3), pp. 828–844, 2020.
https://pp.bme.hu/ci/article/view/16389

[15] Djerouni, S., Elias, S., Abdeddaim, M., De Domenico, D. "Effectiveness of Optimal Shared Multiple Tuned Mass Damper Inerters for Pounding Mitigation of Adjacent Buildings", Practice Periodical on Structural Design and Construction, 28(1), 04022063, 2023.
https://doi.org/10.1061/(ASCE)SC.1943-5576.0000732

[16] Mylonakis, G., Gazetas, G. "Seismic soil-structure interaction: beneficial or detrimental?", Journal of earthquake engineering, 4(3), pp. 277–301, 2000.
https://doi.org/10.1080/13632460009350372

[17] Mekki, M., Elachachi, S. M., Breysse, D., Nedjar, D., Zoutat, M. "Soil-structure interaction effects on RC structures within a performance-based earthquake engineering framework", European Journal of Environmental and Civil Engineering, 18(8), pp. 945–962, 2014.
https://doi.org/10.1080/19648189.2014.917056

[18] Oz, I., Senel, S. M., Palanci, M., Kalkan. A. "Effect of soil-structure interaction on the seismic response of existing low and mid-rise RC buildings", Applied Sciences, 10(23), 8357, 2020.
https://doi.org/10.3390/app10238357

[19] Arboleda-Monsalve, L. G., Mercado, J. A., Terzic, V., Mackie, K. R. "Soil–structure interaction effects on seismic performance and earthquake-induced losses in tall buildings", Journal of Geotechnical and Geoenvironmental Engineering, 146(5), 04020028, 2020.
https://doi.org/10.1061/(asce)gt.1943-5606.0002248

[20] Liu, S., Li, P., Zhang, W., Lu, Z. "Experimental study and numerical simulation on dynamic soil-structure interaction under earthquake excitations", Soil Dynamics and Earthquake Engineering, 138, 106333, 2020.
https://doi.org/10.1016/j.soildyn.2020.106333

[21] Kaveh, A., Ardebili, S. R. "A comparative study of the optimum tuned mass damper for high-rise structures considering soil-structure interaction", Periodica Polytechnica Civil Engineering, 65(4), pp. 1036–1049, 2021.
https://doi.org/10.3311/PPci.18386

[22] Sobhi, P., Far, H. "Impact of structural pounding on structural behaviour of adjacent buildings considering dynamic soil-structure interaction", Bulletin of Earthquake Engineering, 20, pp. 3515–3547, 2022.
https://doi.org/10.1007/s10518-021-01195-w

[23] Mahmoud, S., Abd-Elhameed, A., Jankowski, R. "Behaviour of colliding multi-storey buildings under earthquake excitation considering soil-structure interaction", Applied Mechanics and Materials, pp. 166–169, pp. 2283–2292, 2012.
https://doi.org/10.4028/www.scientific.net/AMM.166-169.2283

[24] Pawar, P. D., Murnal, P. B. "Effect of seismic pounding on adjacent blocks of unsymmetrical buildings considering soil-structure interaction", International Journal of Emerging Technology and Advanced Engineering, 4(7), pp. 391–395, 2014.

[25] Mahmoud, S., Abd-Elhamed, A., Jankowski, R. "Earthquake-induced pounding between equal height multi-storey buildings considering soil-structure interaction", Bulletin of Earthquake Engineering, 11, pp. 1021–1048, 2013.
https://doi.org/10.1007/s10518-012-9411-6

[26] Miari, M., Jankowski, R. "Analysis of pounding between adjacent buildings founded on different soil types", Soil Dynamics and Earthquake Engineering, 154, 107156, 2022.
https://doi.org/10.1016/j.soildyn.2022.107156

[27] Miari, M., Jankowski, R. "Incremental dynamic analysis and fragility assessment of buildings founded on different soil types experiencing structural pounding during earthquakes", Engineering Structures, 252, 113118, 2022.
https://doi.org/10.1016/j.engstruct.2021.113118

[28] Tena-Colunga, A., Sánchez-Ballinas, D. "Required building separations and observed seismic pounding on the soft soils of Mexico City", Soil Dynamics and Earthquake Engineering, 161, 107413, 2022.
https://doi.org/10.1016/j.soildyn.2022.107413

[29] Richart, Jr, F. E., Whitman, R. V. "Comparison of footing vibration tests with theory", Journal of the Soil Mechanics and Foundations Division, 93(6), pp. 143–168, 1967.
https://doi.org/10.1061/JSFEAQ.0001049

[30] Mahmoud, S., Jankowski, R. "Modified linear viscoelastic model of earthquake-induced structural pounding", [pdf] Iranian Journal of Science and Technology, Transactions of Civil Engineering, 35(C1), pp. 51–62, 2011. Available at: https://www.sid.ir/EN/VEWSSID/J_pdf/8542011C101.pdf

[31] Anagnostopoulos, S. A. "Equivalent viscous damping for modeling inelastic impacts in earthquake pounding problems", Earthquake Engineering and Structural Dynamics, 33(8), pp. 897–902, 2004.
https://doi.org/10.1002/eqe.377

[32] Mekki, M., Elachachi, S. M., Breysse, D., Zoutat, M. "Seismic behavior of R.C. structures including soil-structure interaction and soil variability effects", Engineering Structures, 126, pp. 15–26, 2016.
https://doi.org/10.1016/j.engstruct.2016.07.034

[33] Mekki, M., Hemsas, M., Zoutat, M., Elachachi, S. M. "Effects of soil-structure interaction and variability of soil properties on seismic performance of reinforced concrete structures", Earthquakes and Structures, 22(3), pp. 219–230, 2022.
https://doi.org/10.12989/eas.2022.22.3.219

[34] Beer, M., Ferson, S. Kreinovich, V. "Imprecise Probabilities in Engineering Analyses", Mechanical Systems and Signal Processing, 37(1–2), pp. 4–29, 2013.
https://doi.org/10.1016/j.ymssp.2013.01.024

[35] Kaveh, A., Kalateh-Ahani, M., Fahimi-Farzam, M. "Constructability optimal design of reinforced concrete retaining walls using a multi-objective genetic algorithm", Structural Engineering and Mechanics, 47(2), pp. 227–245, 2013.
https://doi.org/10.12989/sem.2013.47.2.227

[36] Kaveh, A., Hoseini Vaez, S. R., Hosseini, P., Fathali, M. A. "Heuristic operator for reliability assessment of frame structures", Periodica Polytechnica Civil Engineering, 65(3), pp. 702–716, 2021.
https://doi.org/10.3311/PPci.17580

[37] Mekki, M., Zoutat, M., Elachachi, S. M., Hemsas, M. "Sensitivity analysis of uncertain material RC structure and soil parameters on seismic response of soil-structure interaction systems", Periodica Polytechnica Civil Engineering, 66(3), pp. 739–751, 2022.
https://doi.org/10.3311/ppci.20113

[38] Jankowski, R., Mahmoud, S. "Earthquake-induced structural pounding", Springer, 2015. ISBN: 978-3-319-35829-1
https://doi.org/10.1007/978-3-319-16324-6